Available online at www.sciencedirect.com

ScienceDirect

Ceramics International 40 (2014) 9367–9375

CERAMICS INTERNATIONAL

www.elsevier.com/locate/ceramint

Experimental determination of the uniaxial viscosity of low-temperature co-fired ceramic tapes by vertical sintering

Liangping Yu, Shishun Qi, Zhaosheng Ma, Ruzhong Zuo*

Institute of Electro Ceramics & Devices, School of Materials Science and Engineering, Hefei University of Technology, Hefei 230009, China

Received 3 January 2014; accepted 2 February 2014
Available online 18 February 2014

Abstract

This paper reports the experimental determination of the uniaxial viscosity for ceramic tapes made of three commercially available low-temperature cofired ceramic (LTCC), DuPont 951 (glass–ceramic), Ferro A6M (glass) and Yinfeng 8.5 (glass) by utilizing a novel vertical sintering in an optical dilatometer. The green tapes were vertically sintered at different isothermal temperatures ranging from 760 °C to 820 °C under their own weights. The densification behavior was systematically investigated through the measured sintering strains and the uniaxial viscosity was determined as a function of relative density based on a theoretical equation developed for ceramic tapes. The calculated uniaxial viscosities were compared with a previously reported model and good agreements were achieved. The activation energy for the uniaxial viscosity was found to be independent of the relative density and showed an average value of 290 ± 47 kJ/mol for the DuPont tapes but was not accessible currently for the other glass-based LTCC tapes.

Keywords: Ceramics tapes; Viscosity; LTCC; Vertical sintering

1. Introduction

The low temperature cofired ceramic (LTCC) tapes have been widely applied as the basic component in the miniaturized devices, providing benefits that include low cost, design flexibility, reliability and size reduction [1–4]. However, in the integration process, mismatched densification kinetics among tapes would lead to undesired defects, such as circuit damage, inaccurate element alignment, shape distortion, cracks and warpage, which would result in the performance degradation of the integrated products [5–9]. To investigate the reason for the above defects, it is necessary to get a deep understanding of the underlying sintering mechanisms for the LTCC tapes.

Usually, the sintering behavior could be regarded as the response of the green body to the sintering pressure. By assuming the sample is isotropic, the sintering behavior could be described from a macroscopic point of view by using continuum mechanical equations based on the visco-elastic theory, which was further demonstrated by Bordia and Sherer using a viscous analog [10,11]. Most LTCC materials are composed of crystallizable glass or glass matrix with ceramic particle fillers and the sintering behavior has been analyzed based on the constitutive equations [12–14]. Thus, knowledge of material's sintering parameters such as the uniaxial viscosity (abbreviated as E_p) and how it evolves during the sintering process, is essential in predicting the sintering behavior of integrated LTCC tapes. Up to date, the E_p has been repeatedly investigated both theoretically and experimentally [14–19]. Experimental determination of sintering parameters is essential for the optimal sintering process and the E_p is usually obtained by measuring strain rates at an applied stress. Valid experimental techniques including discontinuous sinter forging and cyclic loading dilatometry have been successfully applied for the E_p measurement in bulk LTCC materials [3,18,19]. However, the above-mentioned analytical techniques seem not to be applicable to the direct measurement of the E_p for ceramic tapes, which would break easily under load during the dilatometric measurement mainly due to the large ratio of in-plane dimension to the thickness [20]. Up to date, only few

*Corresponding author. Tel./fax: +86 551 62905285.
E-mail address: piezolab@hfut.edu.cn (R. Zuo).

http://dx.doi.org/10.1016/j.ceramint.2014.02.004
0272-8842

attempts have been adopted in the direct determination of sintering parameters for ceramic tapes. The sintering pressure of a ceramic tape was determined by Raj by utilizing a tensile load, but the anisotropic structure was ignored [21]. A beam-bending test together with a non-contact video imaging system was also adopted by Lee et al. to measure the E_p of porous beam material during sintering [22]. Recently, a novel vertical sintering method was proposed by Cologna et al. and it was successfully applied in the measurement of the E_p for several kinds of ceramic tapes, such as yttria-stabilized zirconia (YSZ) tapes, gadolinium-doped cerium oxide (CGO) tapes and lanthanum strontium manganate (LSM) tapes [20,23]. In this method, the tapes were vertically aligned and sintered under the load of their own weight. And the E_p could be determined through the strain rate difference induced by a small tensile stress from the tape's weight. It has also been demonstrated that the microstructure for the vertically sintered tapes was not influenced by the tape's weight [20,23]. However, there has been no trial on the direct measurement of the E_p for LTCC tapes, although they are widely applied in the integration process.

Herein, we report the successful determination of the E_p for three LTCC tapes by utilizing the novel vertical sintering method. The densification behavior of DuPont 951 Tape™, Ferro A6M™ tapes, and Kunming Yinfeng 8.5™ tapes were systematically studied. The Dupont 951 material was a glass–ceramic system and the FE and YF materials were crystalizable glass systems. The approach adopted here could be further applied to other LTCC tapes for the direct determination of the E_p. The dimensions of the tapes were recorded through an in-situ optical dilatometer which could be used to determine the sintering strains. Furthermore, strain rates as a function of relative density were calculated and the E_p of the three LTCC tapes could be determined through a theoretical equation developed for the vertical sintering case, which was clearly explained in the next section. For DuPont 951 tapes, the activation energy for the E_p was determined through the Arrhenius plots of $\ln(E_p) \sim 1/T$ but not accessible for the Ferro A6M™ tapes, and Kunming Yinfeng 8.5™ tapes in current study. The measured E_p values for the three LTCC tapes were also compared with a previously reported model and a good agreement was achieved.

2. Theory description

Generally, by assuming isotropic microstructures for the sintered samples, the sintering behavior could be described based on the constitutive mechanical Eqs. (1)–(3) [3,10–13]

$$\dot{\varepsilon}_1 = \dot{\varepsilon}_{f1} + \frac{1}{E_p}\left[\sigma_1 - \nu_p(\sigma_2+\sigma_3)\right] \tag{1}$$

$$\dot{\varepsilon}_2 = \dot{\varepsilon}_{f2} + \frac{1}{E_p}\left[\sigma_2 - \nu_p(\sigma_1+\sigma_3)\right] \tag{2}$$

$$\dot{\varepsilon}_3 = \dot{\varepsilon}_{f3} + \frac{1}{E_p}\left[\sigma_3 - \nu_p(\sigma_1+\sigma_2)\right] \tag{3}$$

where E_p and ν_p are the uniaxial viscosity and the viscous poisson's coefficient of a porous sintering body, and $\dot{\varepsilon}_x$ (x=1, 2, 3, $f1$, $f2$, $f3$) is the strain rate in three directions with and without externally applied stress, respectively. And the uniaxial viscosity for a uniaxially loaded sample ($\sigma_1 \neq 0$, $\sigma_2 = \sigma_3 = 0$) could be determined based on the following equation:

$$E_p = \frac{\sigma_1}{\dot{\varepsilon}_1 - \dot{\varepsilon}_{f1}} \tag{4}$$

However, owing to an extremely large ratio of in-plane dimension to the thickness for ceramic tapes, most loading methods applied to the bulk sample could not be directly adopted and the Eq. (4) is not suitable in the determination of the uniaxial viscosity. Therefore, novel methods suitable for ceramic tapes should be developed. Recently, the E_p of ceramic tapes like YSZ, CGO and LSM has been successfully obtained by utilizing a vertical sintering method. In the situation, the tape was hung freely and the only applied mechanical stress was the tape's weight. Previous results have also demonstrated that the anisotropic microstructure would not be induced by the minimal tensile stress in the vertically sintered tapes [20,23]. Therefore, the stress could be applied continuously from the beginning to the end of the sintering cycle.

It has been demonstrated that the sintering behavior of LTCC materials could be treated as linearly viscous. By considering the sintering stress σ_s and its own weight, the strain rate in the vertical direction for the vertically sintered tape could be described as [20]

$$\dot{\varepsilon}_v = \frac{\rho g L}{2E_p} + \frac{\sigma_s(1-2\upsilon_p)}{E_p} \tag{5}$$

And, since

$$\sigma_s = \frac{E_p \dot{\varepsilon}_f}{1-2\upsilon_p} \tag{6}$$

the uniaxial viscosity of a ceramic tape could be determined from the following equation:

$$E_p = \frac{\rho g L}{2(\dot{\varepsilon}_v - \dot{\varepsilon}_{f1})} \tag{7}$$

where $\dot{\varepsilon}_v$ and $\dot{\varepsilon}_{f1}$ are the strain rates in the vertical direction of vertically and freely sintered tapes, respectively, L is the instantaneous length in the vertical direction, and ρ is the instantaneous density of the vertically sintered tape. By assuming an isotropic shrinkage behavior, the relative density of freely sintered sample could be calculated from the linear strain data using the following equation:

$$\rho = \rho_o e^{-3\varepsilon_f} \tag{8}$$

However, the relative density for the vertically sintered tape should be calculated based on the equation

$$\rho = \rho_o e^{-(2\varepsilon_h + \varepsilon_v)} \tag{9}$$

where ρ_0 is the relative density of the green tapes, ε_h and ε_v represent the strains in the horizontal and vertical directions, respectively, $2\varepsilon_h$ was still used in the equation to make the

density data reliable, despite that the sintering strain in the horizontal direction of a vertically sintered sample has been demonstrated to be very close to that of a freely sintered tape [20].

From the above equations, the E_p could be directly determined as a function of relative density based on the experimentally measured strain rate difference in the vertical direction between the freely and vertically sintered tapes. Therefore, two separate sets of experiments are conducted to obtain the data required in the equation. The first one is to obtain the strain rates of freely sintered tapes and the other is to obtain the strain rates of vertically sintered tapes in the vertical direction.

3. Experimental

In this study, LTCC tapes such as DuPont 951 tape™, Ferro A6M™ tape and Yinfeng 8.5 tape were used which were called DU, FE and YF tapes hereafter. DU and FE tapes were commercially received and YF tapes were made via a typical casting process using the ceramic powder ($\varepsilon = 8.5$, Yinfeng New Materials Co., Ltd, Yunnan, China). DU is composed of ceramic filler particle and Pb-borosilicate glass, while FE and YF tapes are crystallizable Ca-borosilicate glass and Ca-aluminumsilicate glass, respectively [24–26].

The thickness of the DU and FE tapes was measured to be around 120 μm and that of the YF tape was about 80 μm. The initial densities were determined to be 61.3%, 48.2%, 44.3% for the DU, FE and YF green tapes, respectively. Both the free and vertical sintering experiments were conducted in air for the three LTCC tapes. For the free sintering case, the tapes were laid on the horizontally placed alumina support. However, a quart glass platform was utilized for the vertical sintering case, which could clamp a small area of the tape to make the tape vertically aligned. The tapes for sintering were cut into a half dumb-bell shape with in-plane dimension of 30 mm × 23 mm, and another 5 mm in the vertical direction was used for the fixture in the vertical sintering case. A sketch of a sintered tape is displayed in Fig. 1(a). To realize the in-situ determination of the sintering strains during the sintering process, an optical dilatometer was utilized as previously reported [27]. The sintering strains for the freely sintered tape was determined through dimension changes in the horizontal direction (indicated as W) and the strains for the vertically sintered tape were determined in the horizontal and vertical directions (indicate as W and L). A recoded image of the vertically sintered tape is shown in Fig. 1(b). The sintering behavior was investigated at different isothermal temperatures. For the isothermal tests, the tapes were first heated to 450 °C at 5 °C/min and held for 1 h to remove the organic compounds. The images were recorded starting from 450 °C till the end of the sintering process and there existed no dimension changes for the studied tapes after soaking at 450 °C for 1 h. Then, the tapes were heated at a ramping rate of 10 °C min^{-1} to the isothermal sintering temperatures, such as 760 °C, 780 °C, 800 °C and 820 °C and held for another 4 h. Such long soaking time was used to assure a wide range of density for the obtained E_p. To determine the sintering strains of the ceramic tapes, the dimensions of the freely and vertically sintered tapes were recorded by the in-situ optical dilatometer at 60 s intervals with a resolution of about 4 μm. The sintering strains and densification curves could be obtained by calculating the dimensional changes measured from the recorded images. The relative density was calculated from the strains obtained from the free and vertical sintering process using Eqs. (8) and (9).

To characterize the microstructure of the investigated LTCC tapes, freely and vertically sintered tapes with the same density were used. To minimize the influence of edge effect, the central part in the tape's plane was selected for the following polishing process. Each piece of tape was ground and polished to a 1 μm finish. The polished surfaces of the tapes were then coated with a thin gold conductive layer for the examination of the pore morphology by a scanning electron microscope (SEM, SSX-550, Shimadzu, Japan). The length and angle of pores in the SEM image were determined through the image software (Adobe Photoshop CS6). Then, the pore orientation was obtained by analyzing the statistical data acquired from the images. By comparing the pore orientation, the microstructure could be determined to be isotropic or anisotropic for the vertically sintered tapes.

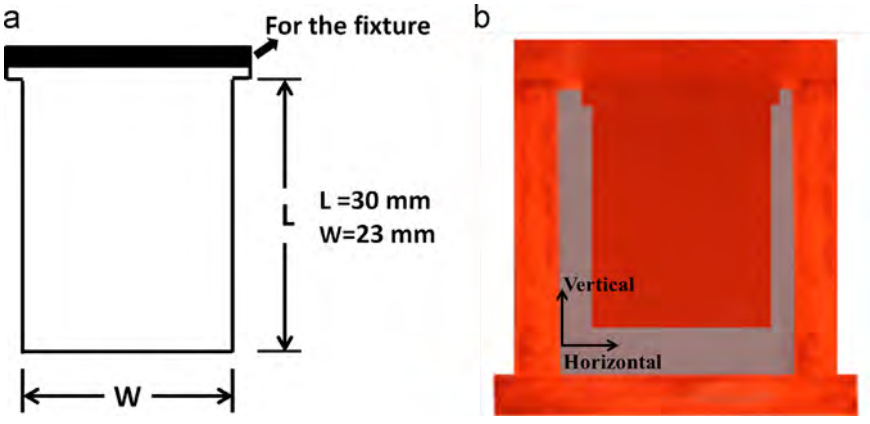

Fig. 1. (a) Schematic illustration for the dimension of the tapes used in free (F) and vertical (V) sintering. (b) Photograph of a vertically hung tape sintered at 800 °C.

4. Results and discussions

Both free and vertical sintering experiments were conducted for DU, FE and YF tapes. The calculated strain data for the samples isothermally treated at different temperatures are shown in Fig. 2. The true strain was used in the calculation of all sintering strains because of the large deformation involved in sintering; i.e., $\varepsilon_L = \ln(L_t/L_o)$, $\varepsilon_H = \ln(W_t/W_o)$, where L_0, W_0, and L_t, W_t are the original and instantaneous lengths of the tape in the vertical and horizontal directions, respectively. Owing to the tensile stress from the tape's weight, it can be deduced that the sintering strain might be reduced in the vertical direction, but was most probably increased in the horizontal direction. However, previous reports suggested that the strain in the horizontal direction of a vertically sintered tape was nearly equal to that of a freely sintered tape [20]. This assumption would affect the calculation precision of the

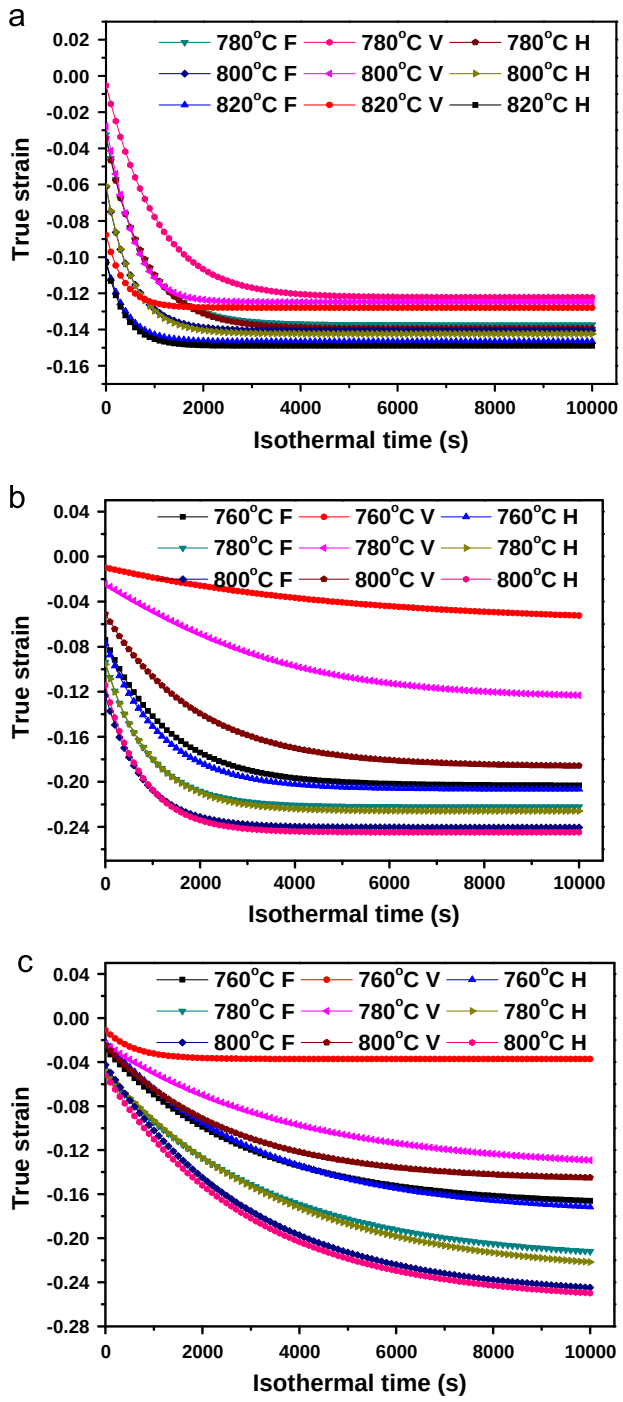

Fig. 2. Sintering strains as a function of the isothermal time: (a) DU tapes at 780 °C, 800 °C and 820 °C, respectively. (b) FE and (c) YF tapes at 760 °C, 780 °C and 800 °C, respectively.

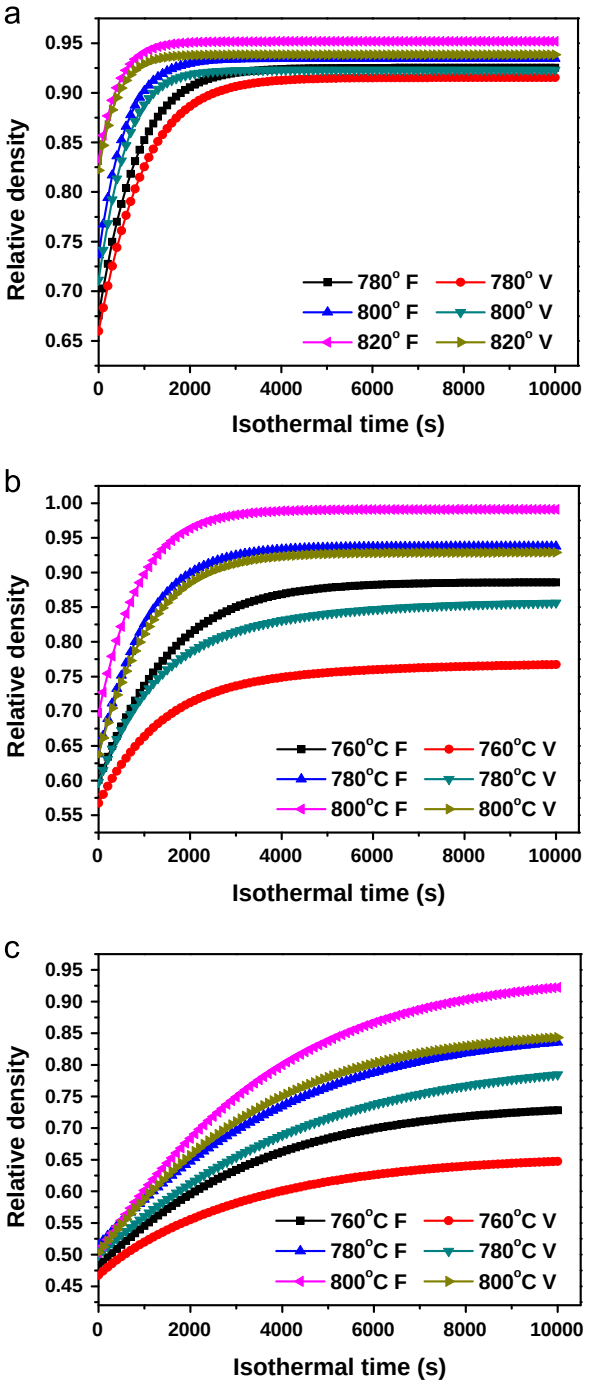

Fig. 3. (a) Relative densities as a function of the isothermal time for freely (F) and vertically (V) sintered ceramic tapes: (a) DU tapes at 780 °C, 800 °C and 820 °C, respectively. (b) FE and (c) YF tapes at 760 °C, 780 °C and 800 °C, respectively.

sintering density hereafter [23]. Therefore, the actual horizontal strains were measured in this study and used in Eq. (9) for the density determination of the tapes. Fig. 3 shows the calculated density data of both freely and vertically sintered DU, FE and YF ceramic tapes based on the strain data in Fig. 2. It could be clearly detected from Fig. 2 that the strains increased with elevating the sintering temperature for all the sintered tapes and the strains in the vertical direction for the vertically sintered tapes were smaller than those of the freely sintered tapes. As can be also observed in Fig. 2, there was only a small deviation between the horizontal strains and free sintering strains and the result was consistent with previous reports [23], which implies that the sintering behavior of the ceramic tape in the horizontal direction was not remarkably affected by a small tensile stress [23]. As shown in Fig. 3, the relative density increased at elevated temperatures and the density value of the freely sintered tapes was higher than that of the vertically sintered tapes. For both the freely and vertically sintered tapes, the density increased with elevating the isothermal sintering temperatures, indicating that the densification behavior was closely related with the isothermal temperature. And the reason for the promoted densification process at relatively higher temperatures could be attributed to the fact that the mobility of the viscous flow was enhanced, which could promote the rearrangement of particles and the growth of necks between particles. The difference of the final density of the freely and vertically sintered tapes could be assigned to the weight of the tape, which plays a role like a tensile stress and impedes the densification process.

Moreover, it could be also observed from Figs. 2 and 3 that the differences of strain and density between the freely and vertically sintered tapes in DU tapes were smaller than those in FE and YF tapes. That is to say, the tape's own weight had minor influence in the vertically sintered DU tapes compared with the FE and YF tapes. The reason for this difference could be ascribed to the different density at the start of the isothermal sintering and the different densification process. As seen in Fig. 3, the initial density for the DU tapes was higher than that of the FE and YF tapes, which would lead to much higher resistance to the tape's own weight. The DU system is composed of ceramic fillers and glass, being densified based on a viscous sintering mechanism. However, the FE and YF tapes were composed of the crystallizable glass, being involved in a complex chemical reaction and a viscous sintering. The different densification process involved in the sintering would result in different densification behavior for the currently studied tapes.

Fig. 4 shows the strain rate data as a function of density for the three LTCC tapes under both free and vertical sintering, which were obtained by fitting exponential function to the strain vs. time curves in Fig. 2 in combination with the density values shown in Fig. 3. It can be observed that a large strain rate difference between the freely and vertically sintered samples existed in the initial low-density region and the difference became smaller with the increase of the sample density. The obvious strain rate difference in the low-density region could be mainly attributed to the relatively low creep

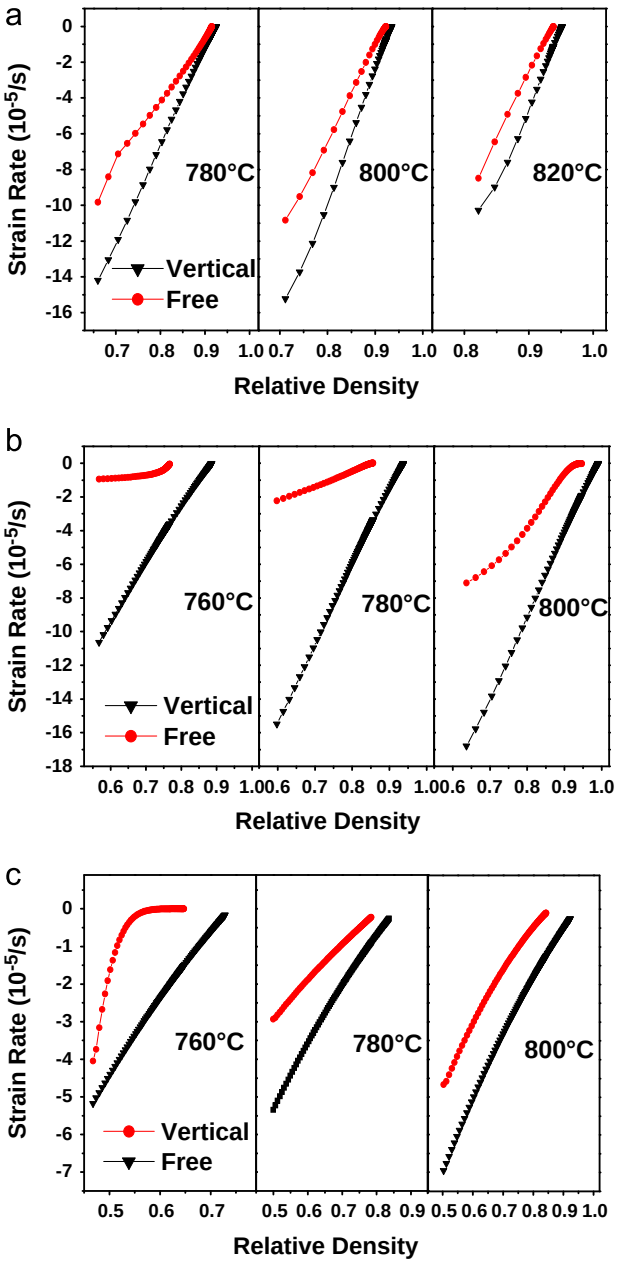

Fig. 4. Sintering strain rate as a function of relative density for freely and vertically sintered ceramic tapes at different isothermal temperatures: (a) DU, (b) FE and (c) YF tapes.

resistance to the tensile stress. It is well known that necks between the ceramic particles are formed in the middle stage of sintering and the growth occurs mainly in the final stage of sintering. In the low-density region, only few necks could exist between the particles, resulting in a small load-bearing area and thus a low resistance to the small tensile stress. However, as the sintering proceeded and density increased, more necks were formed and grown up, which would result in increased load-bearing area and the strain rate difference would become smaller [13,20]. Smaller strain rate differences with increasing sample density could be observed in Fig. 4, which was consistent with the above predictions. Therefore, it is reasonable to conclude that the creep resistance of the LTCC tapes

should be enhanced with increasing density, which might lead to the increase of the E_p. To determine the E_p values for the tapes, Eq. (7) could be applied based on the data shown in Fig. 4.

However, an isotropic microstructure of the sintered tape was an implied essential precondition for the use of Eq. (7). It has been reported that the anisotropic microstructure did not appear in the vertically sintered YSZ, CGO and LSM tapes [20,23]. To confirm the isotropic microstructure in currently studied LTCC tapes, microstructures of the LTCC tapes were examined by employing SEM. By comparing the SEM images of freely and vertically sintered YF tapes at a same density of 84% in Fig. 5(a) and (b), it can be seen that no obvious microstructure difference could be observed. That's to say, the structure of the pores in the vertically sintered tapes was hardly influenced by their own weights. To quantitatively describe the pore orientation, the long axis of each pore in combination with the corresponding angel of this axis to the horizontal direction (indicated in Fig. 5, gravity angle is 90° and 270°) was used. Tens of SEM images with three hundred pores were

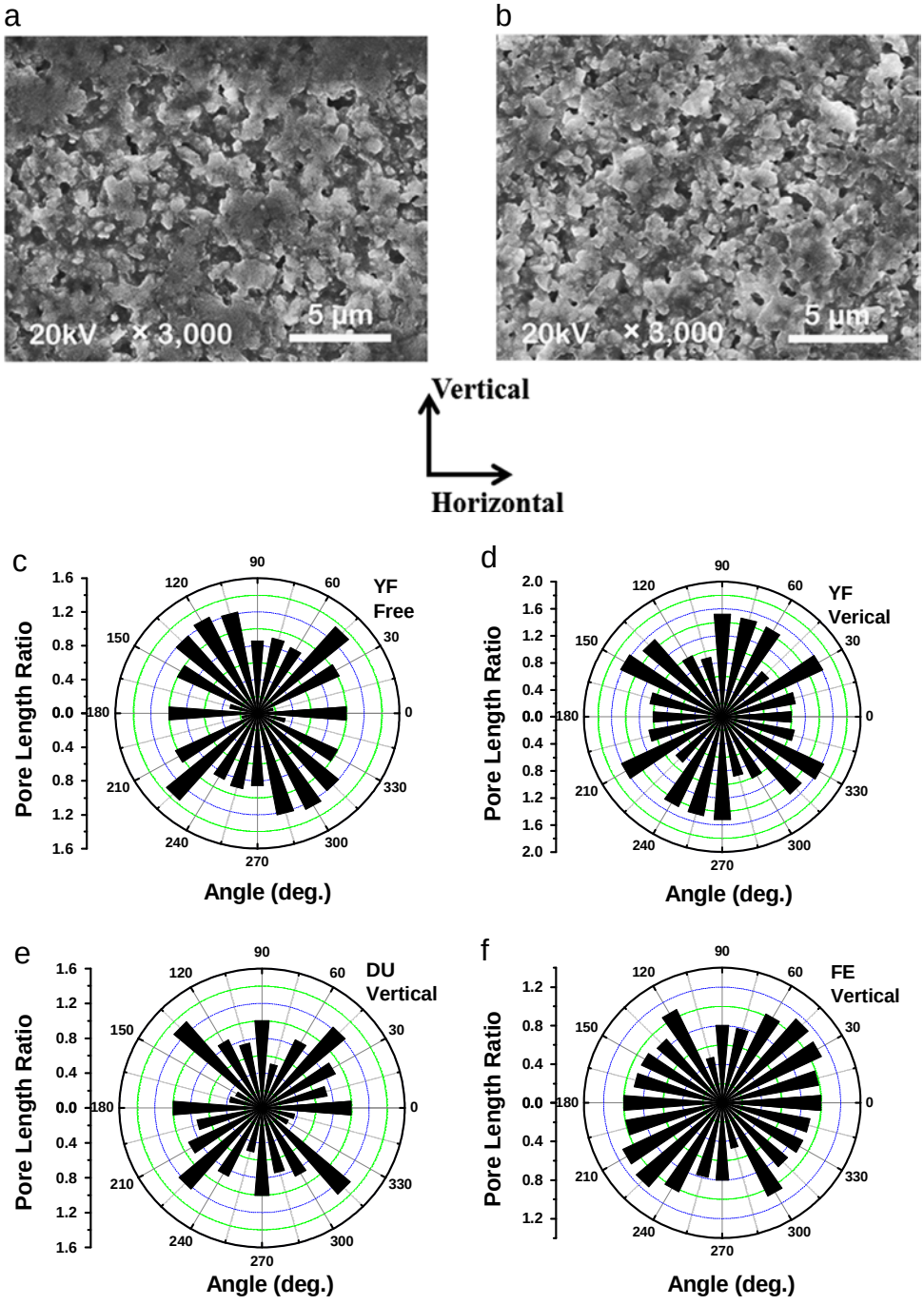

Fig. 5. The SEM images of the YF tapes (a) freely sintered and (b) vertically sintered at 780 °C, and qualitative analysis of the pore orientation for (c) the freely sintered YF tapes, and (d–f) the vertically sintered YF tapes, DU tapes and FE tapes, respectively.

examined and the acquired data was used for the pore orientation analysis. The length of the pores in the same angular segment was added together and then the cumulated lengths at different angular segments were divided by the length near the angle of 0°. The obtained length ratio was used as the radial coordinates, from which a clear comparison of the pore length could be observed. The pore orientations of the freely and vertically sintered YF tapes are displayed in Fig. 5(c) and (d). As observed in Fig. 5(c), the pores in the freely sintered tape were randomly orientated, which was a typical characteristic of an isotropic microstructure. And the isotropic microstructure of the vertically sintered YF tapes could be also confirmed based on the pore orientation result in Fig. 5(d). The results indicated that the microstructure was not influenced by a small tensile stress in vertical sintering cases. The same results could be also found in the vertically sintered DU and FE tapes, as shown in Fig. 5(e) and (f). Therefore, Eq. (7) could be effectively utilized in the calculation of the E_p for the currently studied LTCC tapes.

By using the strain rate difference shown in Fig. 4, the calculated uniaxial viscosities of the studied tapes as a function of their relative densities are shown in Fig. 6. At each isothermal temperature, the E_p could be only calculated in a limited density range and the E_p value in the final stage of densification could not be accurately evaluated with the present method, due to the fact that the small tensile load (its gravity) could not induce any appreciable strain rate difference. It can be clearly seen that the E_p curve for the three materials varied in a non-linear relation with the relative density. At a fixed isothermal temperature, the E_p was relatively low in the low-density region but increased fast as the density increased. The low E_p values observed in the low-density region could be assigned to the small necks between ceramic particles or glass powders and thus a small load-bearing area. The E_p increased rapidly as the densification proceeded, mainly as a result of the development of the inter-particle neck and thus the increase of the load-bearing area [13]. However, when compared at a fixed

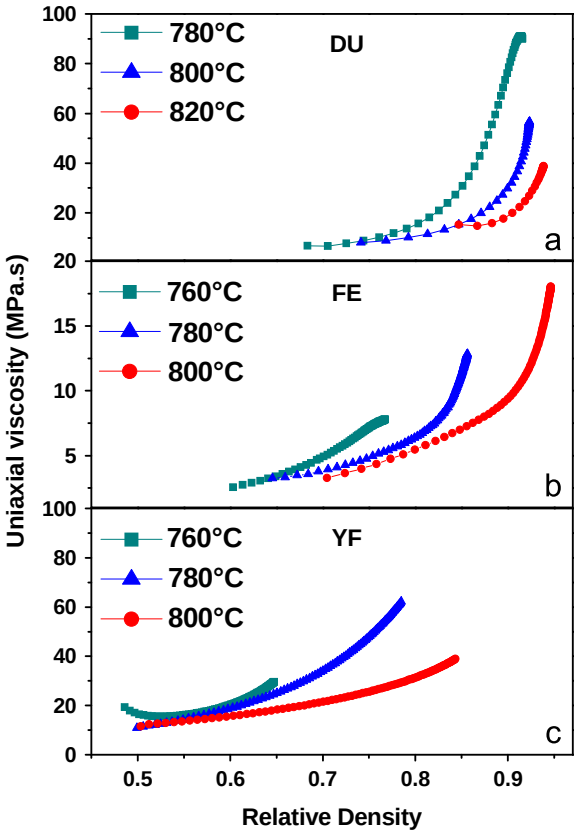

Fig. 6. The uniaxial viscosity as a function of relative density for (a) DU, (b) FE and (c) YF tapes sintered at different isothermal temperatures.

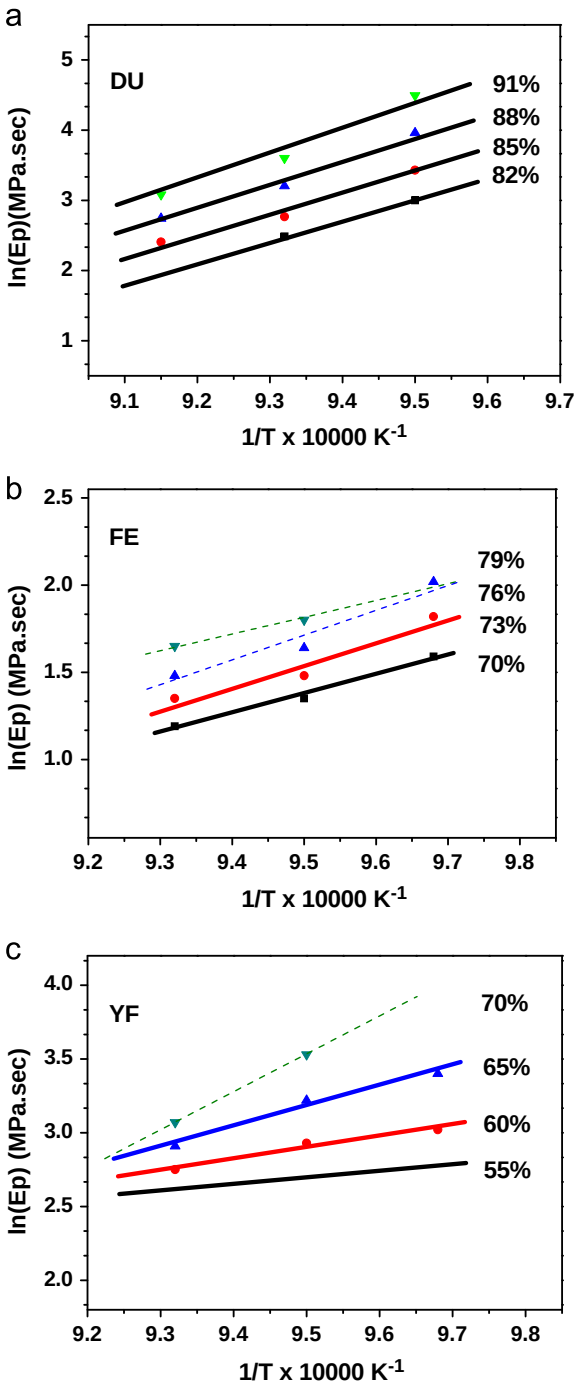

Fig. 7. The Arrhenius plots ($\ln(E_p) \sim 1/T$) of (a) DU tapes, (b) FE tapes and (c) YF tapes.

density, the E_p value increased with decreasing isothermal temperature for the three studied tapes, which could be probably related to the grain growth in the ceramic tapes. It has been reported that the rapid grain growth in the final stage of sintering would contribute to the obvious increase of the viscosity [28].

Since both creep and densification are thermally activated processes, the uniaxial viscosity for the DU tapes could be described by the following equation [13]:

$$E_p = f(\rho)e^{Q_\eta/RT} \tag{10}$$

where Q_η is the activation energy for the uniaxial viscosity, R is the gas constant and T is the absolute temperature. Therefore, the activation energy for the E_p could be determined from the Arrhenius plots of $\ln(E_p) \sim 1/T$ at certain densities, as shown in Fig. 7. For the DU tapes, the $\ln(E_p)$ values were selected at fixed relative densities of 82%, 85%, 88% and 91%. It can be seen from Fig. 7(a) that there exists an almost linear relationship at several different densities and the lines are almost parallel to each other, suggesting that the activation energy of the E_p is nearly independent on density for the DU tapes. The activation energy Q_η value was determined to be 290 ± 47 kJ/mol. Plots of the $\ln(E_p)$ against $1/T$ for the FE and YF tapes are shown in Fig. 7(b) and (c), which were selected at different relative densities. However, it can be obviously observed that the plots for the two kinds of tapes did not exhibit any obvious linear relationship. Moreover, the fitted lines for the plots intersected at some points, which would result in large errors for the determination of activation energy value. Therefore, the activation energy for the E_p of the FE and YF tapes was not accessible since they were crystallizable-glass based systems, which are usually involved in viscous sintering mechanism together with a complex chemical reaction [13]. Hence, more experimental data as well as the phase contents at different temperatures were needed, which was beyond the present work.

A number of theoretical models have been proposed to describe the viscosity–density relation. However, the currently investigated LTCC systems could be only compared with some models based on a viscous sintering mechanism. A well-developed model proposed by Raj et al. was built based on the sintering behavior of glass powder [29]. For comparison, all E_p values were normalized by an initial E_p value at the onset of isothermal sintering (ρ_{iso} at $\rho/\rho_t = 0.75$ for DU tapes, $\rho/\rho_t = 0.705$ for FE tapes and $\rho/\rho_t = 0.56$ for YF tapes) in order to eliminate the effect of the sintering temperatures, where ρ_{iso} is the initial density at the isothermal stage, ρ and ρ_t are the instantaneous density during the isothermal stage and the theoretical density, respectively. The normalized E_p defined as $\overline{E}_p = (E_p(\rho/\rho_t)/E_p(\rho_{iso}))$ for three tapes were plotted as a function of density and compared with the values predicted by the Raj's model, as shown in Fig. 8. It can be found that the Raj's model performed reasonably well in predicting the uniaxial viscosity evolution for the currently studied LTCC tapes. Therefore, the experimental determined E_p values for the three LTCC tapes keep good agreements with the Raj's model.

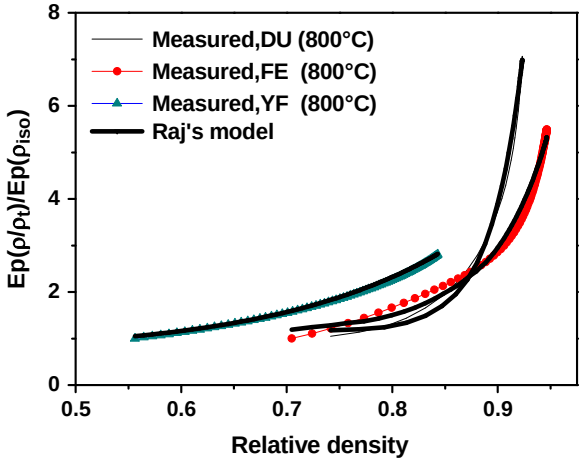

Fig. 8. The normalized uniaxial viscosity $E_p(\rho/\rho_t)/E_p(\rho_{iso})$ as a function of relative density for DU, FE and YF tapes, as compared with the Raj's model [29].

5. Conclusions

The densification behavior of three LTCC tapes made of DU, FE, and YF ceramic was investigated at different isothermal temperatures by means of a lab-made optical dilatometer and their uniaxial viscosities were measured by utilizing a novel vertical sintering method. This approach was realized based on the measurement of the strain rate difference of freely and vertically sintered tapes caused by a continuous but a very low tensile stress, that is, its own weight during the sintering process. The microstructure of the ceramic tapes after free and vertical sintering was carefully examined in order to validate the use of the developed equations. The results could be summarized as follows:

(1) The novel vertical sintering method could be effectively utilized to determine the uniaxial viscosity as a function of relative density for the LTCC tapes based on the fact that isotropic microstructure was verified by the examination of the pore orientation.
(2) For the investigated tapes, the experimentally determined uniaxial viscosities change in a non-linear relation with density, exhibiting a slight increase in the low-density region and a fast rise in the high density region, and show a good agreement with the Raj's model.
(3) The activation energy Q_η of the uniaxial viscosity was computed from the Arrehenius plots for the DU tapes and the value was determined to be 290 ± 47 kJ/mol, and however it was not-available for FE and YF tapes owing to their complex sintering process involved in the glass-based system.

Acknowledgments

This work was financially supported by a Project of the National Natural Science Foundation of China (51272060).

References

[1] A. Mohanram, G.L. Messing, D.J. Green, Densification and sintering viscosity of low-temperature co-fired ceramics, J. Am. Ceram. Soc. 88 (2005) 2681–2689.

[2] D.L. Wilcox, J.W. Burdon, R. Changrani, C.F. Chou, S. Dai, R. Koripella, M. Oliver, D. Sadler, P.V. Allmen, F. Zenhausern, Add ceramic "MEMS" to the pallet of microsystems technologies, Mater. Res. Soc. 687 (2002) 225–242.

[3] J.B. Ollagnier, O. Guillon, J. Rödel, Viscosity of LTCC determined by discontinuous sinter-forging, Int. J. Appl. Ceram. Technol. 3 (2006) 437–441.

[4] R.Z. Zuo, E. Aulbach, J. Rödel, Shrinkage-free sintering of low-temperature cofired ceramic by loading dilatometry, J. Am. Ceram. Soc. 87 (2004) 526–528.

[5] T. Cheng, R. Raj, Flaw generation during constrained sintering of metal–ceramic and metal–glass multilayer films, J. Am. Ceram. Soc. 72 (1989) 1649–1655.

[6] G.Q. Lu, R.C. Sutterlin, T.K. Gupta, Effect of mismatched sintering kinetics on camber in a low-temperature cofired ceramic package, J. Am. Ceram. Soc. 76 (1993) 1907–1914.

[7] J.H. Jean, C.R. Chang, Camber development during cofiring Ag-based low-dielectric-constant ceramic package, J. Mater. Res. 12 (1997) 2743–2750.

[8] P.Z. Cai, D.J. Green, G.L. Messing, Constrained densification of alumina/zirconia hybrid laminates, I: experimental observations of processing defects, J. Am. Ceram. Soc. 80 (1997) 1929–1939.

[9] Y.L. Tung, T.M. Peng, J.H. Jean, S.C. Lin, Stress development during the co-firing of integrated ferrite/dielectric laminates, J. Am. Ceram. Soc. 95 (2012) 946–950.

[10] R.K. Bordia, G.W. Scherer, On constrained sintering: I, constitutive model for a sintering body, Acta Mater. 36 (1988) 2393–2397.

[11] R.K. Bordia, G.W. Scherer, On constrained sintering: II, comparison of constitutive models, Acta Mater. 36 (1988) 2399–2409.

[12] A. Mohanram, S.H. Lee, G.L. Messing, D.J. Green, Constrained sintering of low-Temperature co-Fired ceramics, J. Am. Ceram. Soc. 89 (2006) 1923–1929.

[13] R.J. Xie, R.Z. Zuo, E. Aulbach, U. Mackens, N. Hirosaki, J. Rödel, Uniaxial viscosity of low-temperature cofired ceramic (LTCC) powder compacts determined by loading dilatometry, J. Eur. Ceram. Soc. 25 (2005) 417–424.

[14] R. Raj, R.K. Bordia, Sintering behavior of bi-model powder compacts, Acta Mater. 32 (1984) 1003–1019.

[15] C.H. Hsueh, A.G. Evans, R.M. Cannon, R.J. Brook, Viscoelastic stress and sintering damage in heterogeneous powder compacts, Acta Mater. 34 (1986) 927–936.

[16] E.A. Olevsky, Theory of sintering: from discrete to continuum, Mater. Sci. Eng.: R: Rep. 23 (1998) 41–100.

[17] V.M. Sura, P.C. Panda, Viscosity of porous glasses, J. Am. Ceram. Soc. 73 (1990) 2679–2701.

[18] J.B. Ollagnier, O. Guillon, J. Rödel, Discontinuous sinter-forging of a glass–ceramic composite used in LTCC technology, Int. J. Appl. Ceram. Technol. 3 (2006) 437–441.

[19] A. Mohanram, G.L. Messing, D.J. Green, Measurement of viscosity of densifying glass-based systems by isothermal cyclic loading dilatometry, J. Am. Ceram. Soc. 87 (2004) 192–196.

[20] M. Cologna, V.M. Sglavo, Vertical sintering to measure the uniaxial viscosity of thin ceramic layers, Acta Mater. 58 (2010) 5558–5564.

[21] T. Cheng, R. Raj, Measurement of the sintering pressure in ceramic films, J. Am. Ceram. Soc. 71 (1988) 276–280.

[22] S.H. Lee, G.L. Messing, D.J. Green, Bending creep test to measure the viscosity of porous materials during sintering, J. Am. Ceram. Soc. 86 (2003) 877–882.

[23] D.W. Ni, V. Esposito, C.G. Schmidt, T.T. Molla, K.B. Andersen, A. Kaiser, S. Ramousse, N. Pryds, Camber evolution and stress development of porous ceramic bilayers during co-Firing, J. Am. Ceram. Soc. 96 (2013) 972–978.

[24] S.X. Dai, R.F. Huang, D.L. Wilcox Sr., Use of titanates to achieve a temperature-stable low-temperature cofired ceramic dielectric for wireless applications, J. Am. Ceram. Soc. 85 (2002) 828–832.

[25] A.L. Eustice, S.J. Horowitz, J.J. Stewart, A.R. Travis, H.T. Sawhill, Low-temperature co-fired ceramics: a new approach to electronic packaging, in: Proceedings of the 36th Electronic Components Conference, IEEE, Seattle, New York, 1986, pp. 37–47.

[26] Ferro Corp., Technical publication of ferro tape-A6, Santa Barbara, CA, 1996.

[27] M. Cologna, V.M. Sglavo, M. Bertoldi, Sintering and deformation of solid oxide fuel cells produced by sequential tape casting, Int. J. Appl. Ceram. Technol. 7 (2010) 803–813.

[28] M.N. Rahaman, L.C. DE. Jonghe, R.J. Brook, Effect of shear stress on sintering, J. Am. Ceram. Soc. 69 (1986) 53–58.

[29] V.C. Ducamp, R. Raj, Shear and densification of glass powder compacts, J. Am. Ceram. Soc. 72 (1989) 798–804.